XV International Conference on Atmospheric Electricity, 15-20 June 2014, Norman, Oklahoma, U.S.A.

Large Charge Moment Change Lightning in an Oklahoma Mesoscale Convective System

Timothy J. Lang[1,*], Steven Cummer[2], Danyal Petersen[3], Lizxandra Flores-Rivera[4], Walt Lyons[5], Donald MacGorman[6], and William Beasley[3]

1. National Aeronautics and Space Administration (NASA) Marshall Space Flight Center (MSFC), Huntsville, Alabama, United States of America (USA)
2. Duke University, Durham, North Carolina, USA
3. University of Oklahoma, Norman, Oklahoma USA
4. University of Puerto Rico - Mayaguez, Mayaguez, Puerto Rico, USA
5. FMA Research, Inc., Fort Collins, Colorado, USA
6. National Oceanic and Atmospheric Administration (NOAA) National Severe Storms Laboratory (NSSL), Norman, Oklahoma, USA

ABSTRACT: On 31 May 2013, a line of severe thunderstorms developed during the local afternoon in central Oklahoma, USA. One of the supercells produced the El Reno tornado, which caused significant damage and killed several people. During the 2300 UTC hour (during the mature supercell stage and just after the tornado began), the storm produced several positive cloud-to-ground (+CG) lightning strokes that featured large (> 100 C km) impulse charge moment changes (iCMCs; charge moment during the first 2 ms after the return stroke). These discharges occurred mainly in convection, in contrast to the typical pattern of large-CMC and sprite-parent +CGs occurring mainly in stratiform precipitation regions. After this time, the line of thunderstorms evolved over several hours into a large mesoscale convective system (MCS). By the 0700 UTC hour on 1 June 2013, the large-CMC pattern had changed markedly. Large-CMC negative CGs, which were absent early in the storm's lifetime, occurred frequently within convection. Meanwhile, large-CMC +CGs had switched to occurring mainly within the broad stratiform region that had developed during the intervening period. The evolution of the large-CMC lightning in this case will be examined using a mix of national mosaics of radar reflectivity, the Oklahoma Lightning Mapping Array (OKLMA), the Charge Moment Change Network (CMCN), and the National Lightning Detection Network (NLDN). A major goal of this study is understanding how storm structure and evolution affected the production of large-CMC lightning. It is anticipated that this will lead to further insight into how and why storms produce the powerful lightning that commonly causes sprites in the upper atmosphere.

* Contact information: Timothy J. Lang, NASA MSFC (ZP11), Huntsville, Alabama 35812, USA, email: timothy.j.lang@nasa.gov

INTRODUCTION

Large charge moment change (CMC) lightning has been intimately associated with the production of sprites above thunderstorms. This is due to the high electrical stress exerted on the upper atmosphere by the removal of hundreds (if not thousands) of C km in charge moment by powerful cloud-to-ground (CG) lightning strokes in large storms such as mesoscale convective systems (MCSs) [Lyons et al. 2009]. However, sprite-producing lightning is only a subset of a larger family of rare but powerful lightning, and little is known about the meteorology of all flavors of large-CMC strokes despite the fact that by definition they play a disproportionate role in the global electric circuit. Since modern capabilities allow the detection and geolocation of large-CMC strokes (hereafter assumed to mean > 100 C km, unless otherwise indicated) over the United States [Cummer et al. 2013], recent investigations have started to examine the meteorological context for these events, and an initial hypothesis has been developed [Lang et al. 2013; Beavis et al. 2014]. In storms with normal polarity charge structures (i.e., mid-level negative charge), large-iCMC positive (+) CGs are typically observed to occur in stratiform precipitation regions that are adjacent to strong convection - for example, rearward of the convective line in the commonly occurring leading-line, trailing-stratiform MCS. Most of these flashes would initiate between the mid-level negative and upper positive charge regions in convection, and then escape to the stratiform region while gradually descending (along known advection pathways for charged ice particles; e.g., Carey et al. [2005]) and then finally coming to ground. Meanwhile, large-CMC negative (-) CGs are expected in the convective regions, and also initiate between the upper positive and mid-level negative charge layers. However, instead of traveling into stratiform precipitation they come to ground within convection, and overall have a similar flash structure to a bolt from the blue [Lu et al. 2012].

On 31 May 2013, a line of severe thunderstorms developed during the local afternoon in central Oklahoma, USA. One of the supercells produced the El Reno tornado, a large Enhanced Fujita scale 3 (EF3) multiple vortex tornado that caused significant damage and killed several people, including severe storm researchers Tim and Paul Samaras, and Carl Young [Wurman et al. 2014]. After the supercellular stage, the storm system grew upscale into an enormous MCS that affected several states. Due to its size, severity, duration, and prolific lightning production in range of advanced lightning networks, the storm provided an excellent test case for the previously discussed hypothesis describing large-CMC phenomenology. The results confirm the basic model but also suggest some refinements are necessary.

DATA AND METHODOLOGY

Lightning data for this case came from several different sources. The Oklahoma Lightning Mapping Array (OKLMA) [MacGorman et al. 2008] locates Very High Frequency (VHF) bursts from lightning, enabling the mapping in three-dimensional space plus time. The National Lightning Detection Network (NLDN) [Cummins and Murphy 2009] detects and locates both CG and intra-cloud (IC) lightning. Detection efficiency is very high (> 95%) for CGs, but much lower for ICs. The Duke University Charge Moment Change Network (CMCN) [Cummer et al. 2013] consists of two distantly spaced Extremely Low Frequency (ELF) sensors that measure CMC from CGs that occur within the conterminous United States. NLDN data are used to geolocate these strokes. The CMCN data used for this study provided impulse CMC (iCMC) measurements, or the CMC within the first 2 ms of the return stroke. CGs with iCMCs greater than 100 C km have an approximately ~10% chance to produce a sprite, while iCMCs > 300 C km

are 75-80% likely to produce a sprite [Lyons et al. 2009]. Radar data were provided by the NOAA NSSL Multi-Radar/Multi-Sensor System (MRMS) three-dimensional national radar mosaics [Zhang et al. 2011]. In order to limit the effects of the decline of OKLMA detection efficiency with increasing range, only storms within at most 200 km of the OKLMA centroid were examined.

RESULTS

Overview

Analysis focused on the period from 2000 UTC on 31 May 2013 (before the initiation of any cells) through 1000 UTC the next day (late in the MCS stage of the event, when it was exiting Oklahoma). Figure 1 shows one hour of large-iCMC strokes overlaid on a representative radar mosaic from that time period, early in the lifetime of the El Reno storm. This was during the supercellular stage, and included the time period during which the storm produced the tornado (2303-2343 UTC). There are a number of large-iCMC +CGs (> 100 C km) during the hour, almost all apparently associated with the convective portion of the tornadic supercell, which happened to occur near the center of the OKLMA. There were no large-iCMC -CGs within 200 km of the OKLMA. Many hours later (Fig. 2), the situation had changed. The storm system had grown upscale into a large MCS. Convection along an east-west-oriented line hosted a large number of large-iCMC -CGs, while most large-iCMC +CGs were found to the north in stratiform precipitation, almost all of which were unfortunately out of range of the OKLMA.

Time Series Analysis

Time series for radar and lightning data are shown in Fig. 3. In general, both OKLMA total lightning (Spearman rank correlation coefficient = 0.81) and NLDN total CG lightning (correlation = 0.91) were well correlated with 40-dBZ radar echo volume (Fig. 3a). The reason for the reduced correlation with OKLMA relative to NLDN was twofold. One, the OKLMA's detection efficiency near the effective 200-km limit of its range is greatly reduced while NLDN suffers no such degradation, and two, during the tornado OKLMA total flash rate dropped sharply and remained quasi-steady, before recovering nearly immediately after the tornado lifted. This behaviour appeared to be associated with the presence of a lightning hole (Krehbiel et al. 2000), a common occurrence in thunderstorms with strong updrafts. One might speculate that the strong vorticity associated with the tornado also helped reduce charging via centrifugal ejection of larger hydrometeors from the mesocyclone region. Fig. 3b demonstrates that the storm system was dominated by -CG lightning overall, though its relative fraction declined during the analysis period as the storm grew upscale, developed significant stratiform precipitation area, and moved out of range. This may indicate a combination of reduced flash rates in stratiform regions (Lang and Rutledge 2008) as well as an increasing preference for +CG lightning in those same regions (Rutledge and MacGorman 1988). Despite the -CG dominance, however, large-iCMC lightning was split nearly evenly between the two polarities. There were 101 +CGs with iCMC > 100 C km during the analysis time, compared to 98 -CGs with the same characteristics. The +CG and -CG totals with > 300 C km were 17 and 14, respectively. However, these showed an interesting bimodal behavior, with large-iCMC +CGs favored earlier than large-iCMC -CGs. With both polarities, however, the > 300 C km CGs began to occur only after several hours of > 100 C km activity. Since the storm grew upscale with time, this indicates the

potential effects of lateral growth of charge layers in both convective and stratiform regions.

The OKLMA data were investigated in more detail, in order to better understand the reasons for this large-iCMC behaviour. The storm can be subjectively split into two periods before and after ~0445 UTC. Prior to that time, the mode of OKLMA source density remained mostly below 10 km above mean sea level (MSL; Fig. 4a), and when the storm produced large-iCMC CGs they were mostly positive. After this time, the OKLMA source density mode lifted above 10 km, and the storm began to produce almost exclusively large-iCMC -CGs. Note how, in addition to flash rate, VHF source density also declined during the tornado. Flash areas were computed using the convex hull method similar to Bruning and MacGorman [2013] and displayed along OKLMA flash rate in Fig. 4b. After 0445 UTC, flash rate and median flash area evolved in a quasi-anticorrelated manner, and this latter period was dominated by fewer but larger flashes compared to pre-0445 UTC.

The median altitudes and convex hull areas of OKLMA sources associated with strokes featuring iCMC > 100 C km were examined. In Fig. 5, in order to improve vertical resolution the range limit was reduced to 120 km from OKLMA. This reduced the dataset to 55 +CGs and 18 -CGs. The differences in altitude between the +CGs and the -CGs (Fig. 5a) is striking - the OKLMA-mapped portions of large-iCMC +CGs rarely exceeded 8 km MSL while for -CGs the vertical range was 8-12 km. While large-iCMC +CGs (Fig. 5b) sometimes featured large areas > 500 km^2, the relative fraction of large-iCMC -CGs above that threshold was much greater. The tendency for small-area, large-iCMC +CGs goes against the conventional model of a large-CMC or sprite-parent +CG starting as a convective flash that then propagates up to hundreds of km into stratiform precipitation before coming to ground [Lang et al. 2010]. This discrepancy will be examined later.

The iCMC > 300 C km strokes were examined in a similar manner (Fig. 6). However, due to the small number of flashes the OKLMA range criterion was held at 200 km. This will likely slightly increase source altitudes, increase source altitude uncertainty, as well as reduce the number of sources detected per flash (possibly affecting convex hull areas) [Thomas et al. 2004], although Lang et al. [2010] found that useful flash information can still be extracted beyond 120 km from OKLMA. Despite these issues, the results are very similar to the > 100 C km strokes, except that now both flash polarities featured similarly large convex hull areas (as well as featured large flash-to-flash differences in size for a common polarity).

Radar and Flash Structure

Turning now to individual flashes, a typical example of a large-iCMC +CG is shown in Fig. 7, while a typical large-iCMC -CG is shown in Fig. 8. Much like the flash in Fig. 7, most large-iCMC +CGs were found to occur along the edges of convective cores. Initiation was near mid-levels (~8 km), and lateral propagation was minimal before striking ground. In many of these +CGs, sloped reflectivity structures (Fig. 7c) suggested the possible existence of a tilted dipole [e.g., Carey and Rutledge 1998] that may have exposed positive charge to ground. Alternatively, horizontal heterogeneities in charge structures, caused by the turbulent dynamics of the supercell, may have enabled the formation of short-lived positive charge pockets near mid-levels on the periphery of the thunderstorm core. Both of these interpretations are consistent with the observed -CG dominance (Fig. 3a) and upper-level VHF source maxima (Fig. 4a), which indicated the El Reno storm largely featured a normal polarity electrical structure with predominantly mid-level negative charge. By contrast, typical large-iCMC -CGs (Fig. 8) were much larger

than their +CG counterparts, despite still occurring in, or on the periphery of, convection. The altitude difference is explained by the flash behavior, which suggests a bi-level structure very similar to IC flashes, which then come to ground in a manner similar to bolts from the blue. This hybrid IC/CG behavior in large-iCMC -CGs is very common and suggests that increased altitude is an important contributor to the enhanced charge moment changes [Lu et al. 2012; Lang et al. 2013].

CONCLUSIONS

Late in its lifetime, the large-CMC lightning behavior in the El Reno storm largely fit the emerging model to describe and explain the phenomenology of this powerful sub-class of lightning. To wit, large-CMC negatives occurred mainly in convection and consisted of spatially large hybrid IC/CG flashes with the bulk of their VHF sources occurring at high altitudes. Large-CMC positives were largely confined outside of convection late in the storm's lifetime, unfortunately too far away for OKLMA to map them. Thus, we cannot confirm their likely origin as convective ICs as well, which then escape laterally and come to ground in the stratiform region [Lang et al. 2010]. However, the early portion of this storm does not fit the model. Large-CMC +CGs occurred almost exclusively near convection. This occurred despite the -CG dominance and normal electrical polarity of the storm, so it cannot be ascribed to widespread anomalous electrification [e.g., Wiens et al. 2005]. What was found, however, was that these rare but powerful +CGs occurred on the edges of cores, and thus may have benefitted by transient exposure of positive charge to ground (e.g., tilted dipole) or heterogeneous development of small, short-lived pockets of mid-level positive charge via complex interplay between the turbulent dynamics and the microphysical structure of the supercell. Additional evidence for the latter is the occurrence of a lightning hole that reduced flash rates and VHF source densities during the El Reno tornado.

The switch between this early large-CMC +CG period and the later large-CMC -CG behavior appears to be related to the upscale growth of the storm from a line of supercells to a large MCS. This evolution led to an increase in stratiform precipitation, an overall reduction of flash rates and volume of 40-dBZ reflectivity, a reduction in relative -CG fraction, and an overall increase in flash area (particularly after 0445 UTC). In addition, a greater tendency for > 300 C km CGs to occur was observed as the storm aged, and these "sprite-class" CGs [Beavis et al. 2014] generally propagated over larger areas than their > 100 C km counterparts. During this aging process, after 0445 UTC, VHF source density modes moved to higher altitudes, 10 km MSL or higher, and this was associated with increased large-CMC -CG activity - consistent with the tendency for these powerful flashes to act as hybrid IC/CGs with bolt-from-the-blue characteristics.

Finally, and perhaps most importantly, the results of this analysis clearly show that the behavior of large-CMC lightning (even in more limited form with only impulse-CMC information) is clearly diagnostic of important electrical (and by extension, kinematic and microphysical) changes within thunderstorms. When large-CMC flashes occur, where they occur, and what polarity they are, all likely provide information about thunderstorms that can be exploited to provide additional scientific understanding. Future research to confirm and expand upon all of these findings is planned.

ACKNOWLEDGMENTS

This research is dedicated to the memory of Tim Samaras, his son Paul, and his colleague Carl

Young, all of whom lost their lives in the El Reno tornado. Tim Samaras was a valuable collaborator on the Physical Origins of Coupling to the upper Atmosphere from Lightning (PhOCAL) project, and his contributions are greatly missed. The research presented here is part of PhOCAL, which is run by Duke University and funded by DARPA via the Nimbus program. Ms. Flores-Rivera work on this case was supported by the NASA Marshall summer 2013 internship program and the NASA Lightning Imaging Sensor project. The authors gratefully acknowledge the valuable contributions of the NLDN data from Vaisala, Inc., which enables the geolocation of large charge moment strokes by the CMCN. The views, opinions, and findings in this report are those of the authors, and should not be construed as an official NASA, NOAA, or U.S. Government position, policy, or decision.

REFERENCES

Beavis, N., Lang, T. J., S. A. Rutledge, W. A. Lyons, and S. A. Cummer, 2014: Diurnal, seasonal, and regional behavior of cloud-to-ground lightning with large impulse charge moment changes. *Mon. Wea. Rev.*, Conditionally accepted.

Bruning, E. C., and D. R. MacGorman, 2013: Theory and observations of controls on lightning flash size spectra. *J. Atmos. Sci.*, **70**, 4012–4029.

Carey, L. D., M. J. Murphy, T. L. McCormick, and N. W. S. Demetriades, 2005: Lightning location relative to storm structure in a leading-line, trailing-stratiform mesoscale convective system. *J. Geophys. Res.*, **110**, D03105, doi:10.1029/2003JD004371.

Carey, L. D., and S. A. Rutledge, 1998: Electrical and multiparameter radar observations of a severe hailstorm. *J. Geophys. Res.*, **103**(D12), 13979–14000.

Cummer, S.A., W.A. Lyons, and M.A. Stanley, 2013: Three years of lightning impulse charge moment change measurements in the United States. *J. Geophys. Res.*, **118**, 5176-5189, doi:10.1002/jgrd.50442.

Cummins, K.L. and M.J. Murphy, 2009: An overview of lightning locating systems: History, techniques, and data uses, with an in-depth look at the U.S. NLDN. *IEEE Trans. Elec. Comp.*, **51**(3), 499-518.

Krehbiel, P. R., R. J. Thomas, W. Rison, T. Hamlin, J. Harlin, and M. Davis, 2000: GPS-based mapping system reveals lightning inside storms. *Eos, Trans. Amer. Geophys. Union*, **81**, 21–25.

Lang, T. J., S. A. Cummer, S. A. Rutledge, and W. A. Lyons, 2013: The meteorology of negative cloud-to-ground lightning strokes with large charge moment changes: Implications for negative sprites. *J. Geophys. Res. Atmos.*, **118**, 7886–7896, doi:10.1002/jgrd.50595.

Lang, T. J., W. A. Lyons, S. A. Rutledge, J. D. Meyer, D. R. MacGorman, and S. A. Cummer, 2010: Transient luminous events above two mesoscale convective systems: Storm structure and evolution. *J. Geophys. Res.*, **115**, A00E22, doi:10.1029/2009JA014500.

Lang, T. J., and S. A. Rutledge, 2008: Kinematic, microphysical, and electrical aspects of an asymmetric bow-echo mesoscale convective system observed during STEPS 2000. J. Geophys. Res., 113, D08213, doi:10.1029/2006JD007709.

Lu, G., S. A. Cummer, R. J. Blakeslee, S. Weiss, and W. H. Beasley, 2012: Lightning morphology and impulse charge moment change of high peak current negative strokes. *J. Geophys. Res.*, **117**, D04212, doi:10.1029/2011JD016890.

Lyons, W. A., M. Stanley, J. D. Meyer, T. E. Nelson, S. A. Rutledge, T. J. Lang, and S. A. Cummer, 2009: The meteorological and electrical structure of TLE-producing convective storms. In *Lightning: Principles, Instruments and Applications*, H.D. Betz et al. (eds.), 389-417 pp., Springer Science+Business Media B.V., doi: 10.1007/978-1-4020-9079-0_17.

MacGorman, D. R., and Coauthors, 2008: TELEX: The Thunderstorm Electrification and Lightning Experiment. *Bull. Amer. Meteor. Soc*., **89**, 997–1013.

Rutledge, S. A., D. R. MacGorman, 1988: Cloud-to-ground lightning activity in the 10–11 June 1985 mesoscale convective system observed during the Oklahoma–Kansas PRE-STORM project. *Mon. Wea. Rev.*, **116**, 1393–1408.

Thomas, R. J., P. R. Krehbiel, W. Rison, S. J. Hunyady, W. P. Winn, T. Hamlin, and J. Harlin, 2004: Accuracy of the Lightning Mapping Array. *J. Geophys. Res.*, **109**, doi:10.1029/2004JD004549.

Wiens, K. C., S. A. Rutledge, and S. A. Tessendorf, 2005: The 29 June 2000 supercell observed during STEPS. Part II: Lightning and charge structure. *J. Atmos. Sci.*, 62, 4151-4177.

Wurman, J., K. Kosiba, P. Robinson, and T. Marshall, 2014: The role of multiple-vortex tornado structure in causing storm researcher fatalities. *Bull. Amer. Meteor. Soc.*, **95**, 31–45.

Zhang, J., and Coauthors, 2011: National Mosaic and Multi-Sensor QPE (NMQ) System: Description, results, and future plans. *Bull. Amer. Meteor. Soc.*, **92**, 1321–1338.

FIGURES

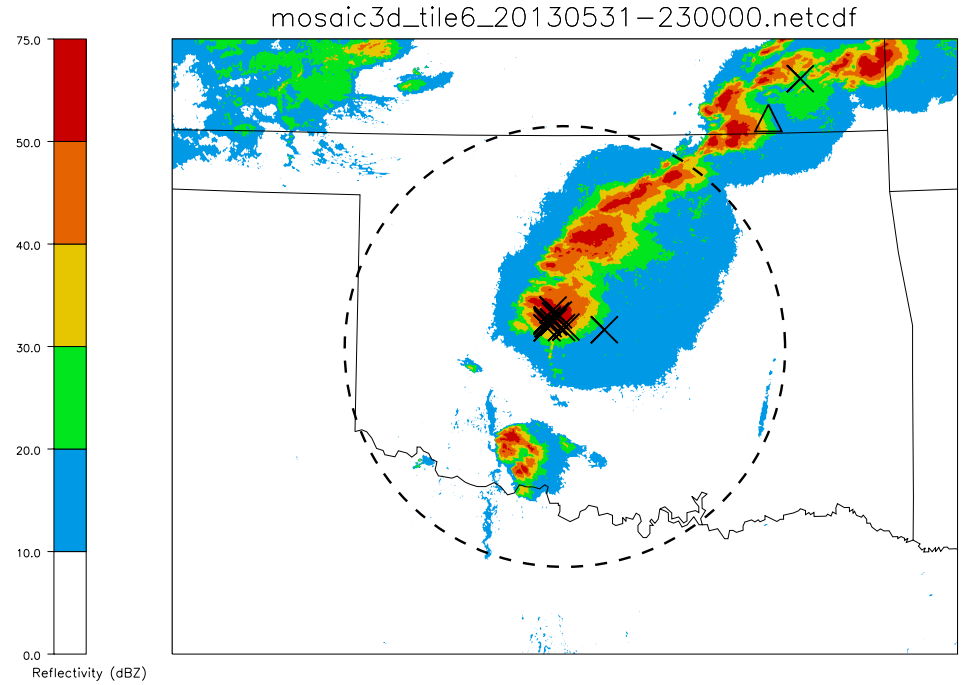

Figure 1. Composite reflectivity at 2300 UTC on 31 May 2013. Also shown are large (> 100 C km) positive iCMCs (Xs) and large negative iCMCs (triangles) that occurred during 2300-0000 UTC (1 h). The dashed ring is 200 km from OKLMA center.

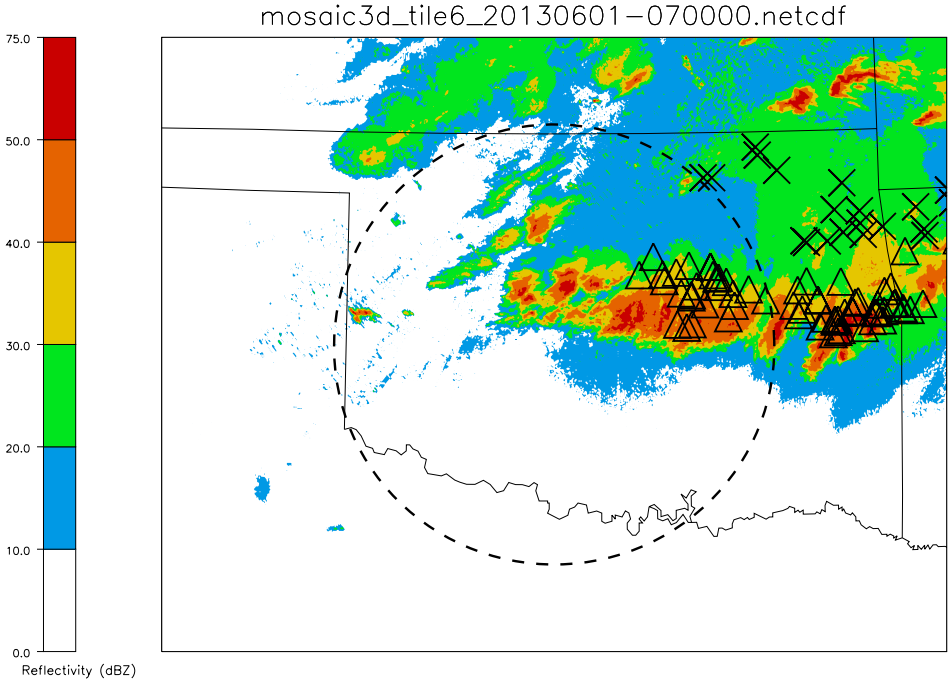

Figure 2. Same as Fig. 1 but for 0700 UTC on 1 June 2013, and with iCMCs during the 0700-0800 hour.

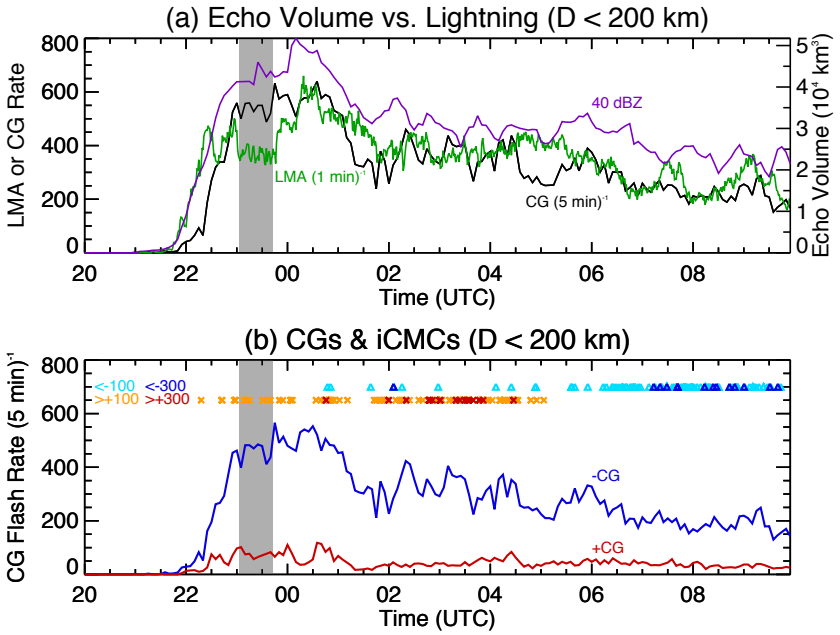

Figure 3. (a) Time series of 40 dBZ echo volume, total CG flash rate, and OKLMA total lightning flash rate within 200 km of the OKLMA center. The shaded region is the time of the El Reno tornado. (b) Similar to (a), but showing positive and negative CG time series. The times of large-iCMC strokes, broken out by 100 and 300 C km thresholds, are indicated above the time series.

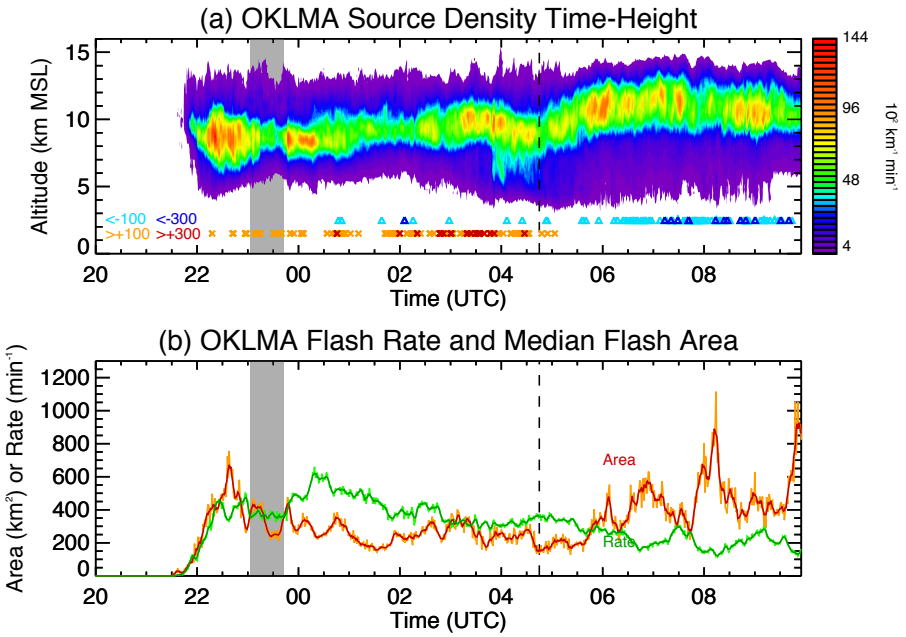

Figure 4. (a) Time-height contour plot of VHF source density from the OKLMA. Also shown are the large-iCMC stroke times as in Fig. 3b. (b) Time series of OKLMA median flash area and total flash rate. The lighter curves are 1-min resolution, while the darker curves are 5-minute running means. The time of the El Reno tornado is shown by

the shaded region in each subplot. The vertical dashed line is used to subjectively indicate where a significant change in lightning behavior began to occur.

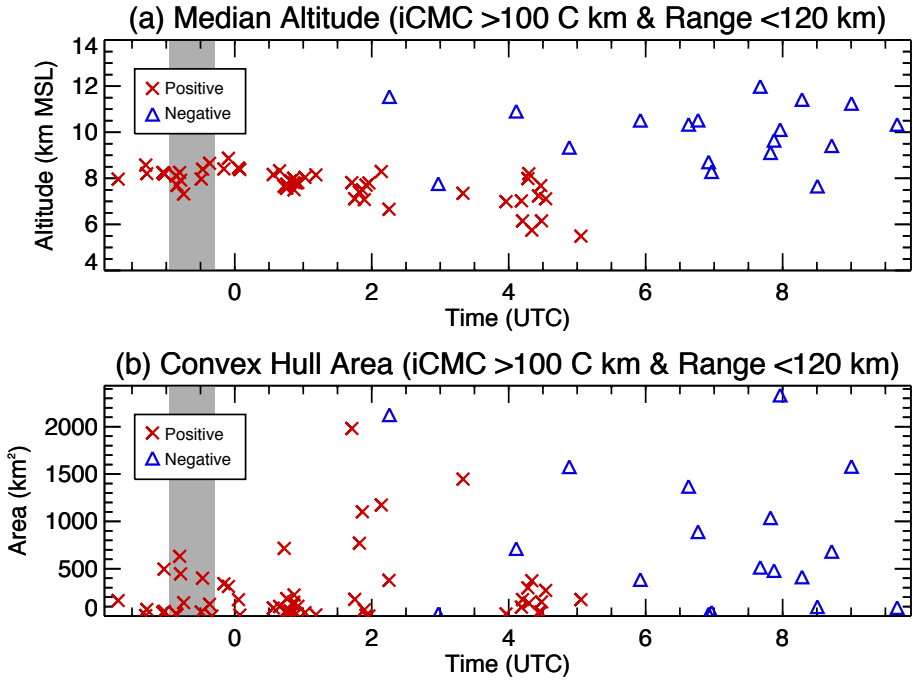

Figure 5. (a) Times and median altitudes of large-iCMC strokes. Thresholds were 100 C km iCMC and 120 km distance from OKLMA. El Reno tornado time is shaded. (b) Similar to (a) but for convex hull flash area.

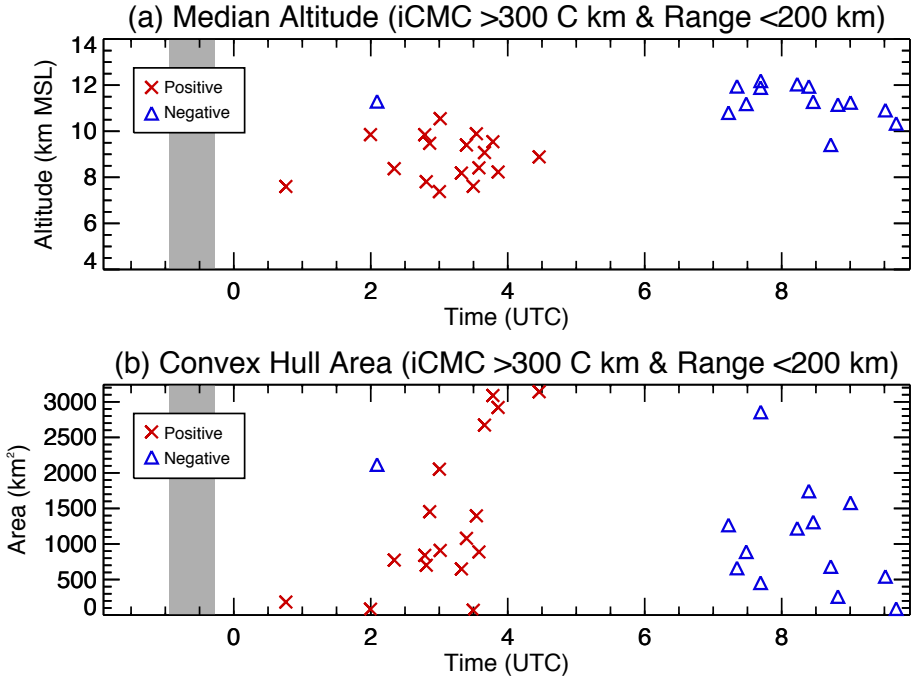

Figure 6. Same as Fig. 5 but now the thresholds are iCMC > 300 C km and OKLMA distance < 200 km.

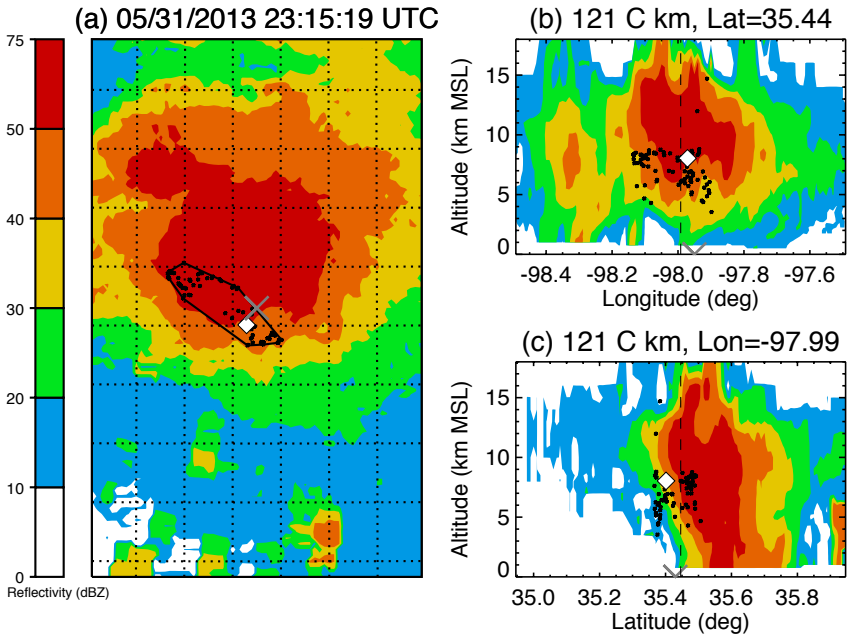

Figure 7. Typical example of a large-iCMC +CG (121 C km). The flash occurred at the indicated time, with radar data coming from 2315 UTC. (a) Plan view with composite radar reflectivity (filled contours), OKLMA sources (black dots), convex hull (black line), flash initiation point (white diamond), and +CG location (gray X). The dotted gridlines are spaced 0.1° apart. (b) Similar to (a), but now a vertical cross-section through the median location of all OKLMA sources, at the indicated constant latitude. (c) Same as (b) but for the indicated constant longitude.

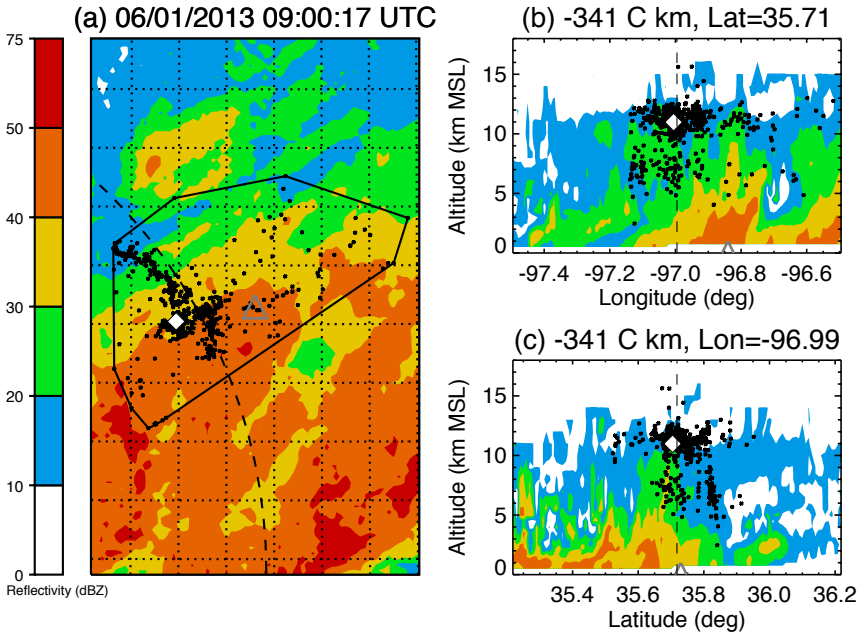

Figure 8. Same as Fig. 7 but now for a typical large-iCMC -CG (-341 C km). The -CG strike is indicated by the gray triangle, and the dashed curve in (a) is part of the 200-km range ring from OKLMA. Radar data are from 0900 UTC.